Self-Diffusion and Viscosity Coefficient of Fluids in Nanochannels

Valery Ya. RUDYAK[1,2*], Alexander A. BELKIN[1,2], Denis A. IVANOV[1,2], Vladimir A. ANDRUSHENKO[1,2]

*Corresponding author: Tel.: +7 383 2668014; Fax: +7 383 2668043; E-mail: valery.rudyak@mail.ru
1: Novosibirsk State University of Architecture and Civil Engineering, Russia
2: Institute of Thermophysics of SB RAS, Novosibirsk, Russia

Abstract Fluid viscosity and molecular diffusion in nanochannels were studied by molecular dynamics simulation. Transport processes in a plane channel, a channel of rectangular cross-section, and in porous media were investigated. The channel height was varied from 2 to 50 nm. The interaction between molecules was simulated using the hard sphere (HS) and the Lennard-Jones (LJ) intermolecular potentials. The porous matrix was modeled by cubic packing of spheres of the same radius, and the packing density and the grain size were varied. The dependence of the transport coefficients on the fluid density and channel characteristics (channel height, channel aspect ratio, porosity of the porous medium, accommodation coefficients, etc.) was investigated.

Keywords: Nanochannel, Self-diffusion, Molecular Diffusion, Viscosity, Porous Medium, Fluid Structure in Nanochannel, Molecular Dynamics

1. Introduction

Flows in microchannels have long attracted the attention of researchers. This is due to the wide occurrence of such flows. They play an important part in many natural phenomena and occur in various natural porous media. In recent decades, interest in microflows has increased because of various technological applications. Transport processes are significant features of fluid flows in microchannels. From a practical point of view, these processes are especially important in porous media. Transport processes in porous media play a great role in everyday human life and various technological processes. Major examples of such processes are heat and mass transfer in living organisms, transport of soil moisture, impurity precipitation on treatment plant filters, acceleration of reactions by porous catalysts, motion of hydrocarbons in collectors, etc.

A key transport process is the self-diffusion of fluid molecules. Molecular self-diffusion is widely used in practice to obtain information on the structure and geometry of the pore space (see, for example, Latour et al., 1993; Song et al., 2000).

For obvious reasons, microflows and especially nanoflows are difficult to study experimentally. At best, it is possible to obtain information on some integral characteristics (flow rate, pressure drop, average velocity, etc.). It is very hard to determine the fluid transport coefficients in microchannels and nanochannels. The greatest success has been achieved in determining diffusion coefficients (see, e.g., a review Kärger & Ruthven, 1992). However, in this case, experimental data have been interpreted using macroscopic theories. The measurement of the viscosity coefficient in microflows and nanoflows is an even more difficult problem. It is necessary to develop new types of viscosimeter for this purpose (see Kang et al., 2010 and references therein).

Because of the difficulties in experimental studies of the transport processes in microflows and nanoflows, it is reasonable to develop alternative simulation methods. The most consistent method of this kind is the molecular dynamics (MD) technique, in which the transport processes are simulated on the basis of the first principles. However, the problem is very complex, and the MD simulation is taking the first steps in this direction. There are few systematic data on the transport coefficients in microflows and

nanochannels and the difference between them and those in the bulk.

In this article, we present an MD simulation study of the fluid viscosity and molecular diffusion in nanochannels. Transport processes in a plane channel, a channel with a rectangular cross-section, and in porous media were investigated. The channel height was varied from 2 to 50 nm. The interaction of molecules was simulated using the hard sphere (HS) and the Lennard-Jones (LJ) potentials. In first case, the hard plates were the walls of the channel. The interaction between the fluid molecules and the channel walls was described by specular, diffuse or specular-diffuse reflection. For LJ fluids, the channel walls were simulated by several rows of cubic packed molecules. The problem was solved using the Schofield scheme.

The porous matrix was modeled by cubic packing of hard spheres of the same radius, and the packing density and grain size were varied. The calculations were performed in a cell with periodic boundary conditions, i.e., in fact, an infinite porous medium was modeled.

The transport coefficients were calculated both by using the Green–Kubo formula in terms of the correlation function and by calculating the mean-square displacement of a molecule along and across the channel. The dependence of the transport coefficients on fluid density and channel characteristics was investigated. Because the transport properties of a fluid depend on its structure, we first consider the fluid structure in nanochannels.

2. Fluid Structure in Nanochannels

Transport processes in nanochannels are determined by two different mechanisms: (i) the interactions of fluid molecules with the channel walls and (ii) interaction of molecules in the bulk. In small channels, the number of molecules interacting with the wall is comparable with the number of molecules interacting in the bulk. Therefore, the fluid structure in nanochannels differs significantly from the fluid structure in macroscopic channels. In particular, the fluid density profile in a nanochannel is inhomogeneous. Density profiles in the channel cross-section for LJ and HS fluids are compared in Fig. 2.1. Here the fluid density is described by the parameter $\varepsilon_V = n\sigma^3$ for a LJ fluid and $\varepsilon_V = nd^3$ for a HS fluid, n is the fluid number density, d is the diameter of the molecule, and σ is the parameter of the LJ potential. A well-defined periodic structure is observed. It is evident that the density has maximum values at the channel walls. The number and height of the maxima increase with increasing fluid density.

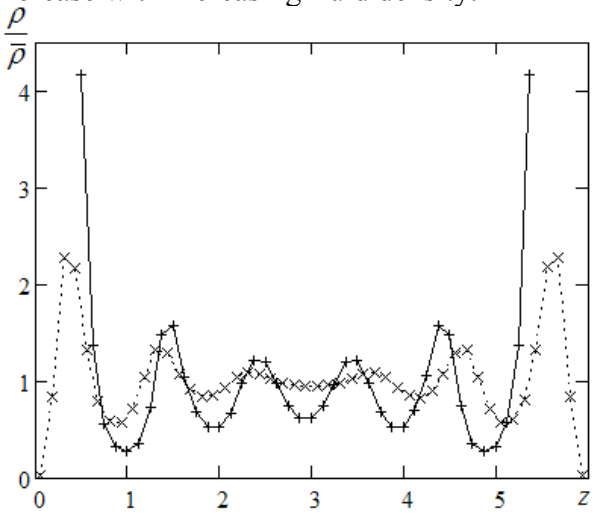

Fig. 2.1. Density profiles across a nanochannel for HS (+), and LJ fluid (×). $L = 60\sigma$, $h = 6\sigma$, $\varepsilon_V = 0.79$

The periodic structure is more pronounced in a HS fluid than in a LJ fluid at the same average density. This is primarily due to the existence of a screening layer at the walls for HS molecules. For LJ molecules, the screening effect is less pronounced because the LJ potential is softer than the HS potential. Because of the existence of screening zones, the effective volume occupied by LJ molecules is larger than that occupied by HS molecules. Therefore, the effective density of a HS fluid is higher than the density of LJ molecules (with the same number of molecules in the modeling cell). However, the fluid structuring in the channel increases with increasing fluid density.

It should be emphasized that the order of the fluid near the walls is a characteristic feature of nanochannel flows, and it does not disappear with increasing distance between the channel walls. This is illustrated in Fig. 2.2, which shows fluid density profiles across

channels of different heights. Fluid structuring in the channel practically does not depend on the channel height if the latter is greater than 10σ. In all cases, appreciable structuring takes place at a distance from the walls of about 5–6σ.

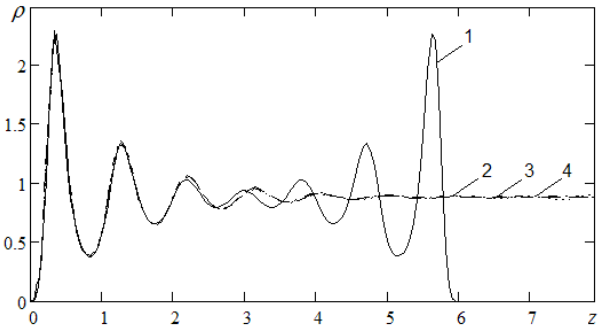

Fig. 2.2. Density profiles for nanochannels of different heights. $\varepsilon_V = 0.88$, 1 – $h = 6\sigma$, 2 – $h = 12\sigma$, 3 – $h = 24\sigma$, 4 – $h = 48\sigma$

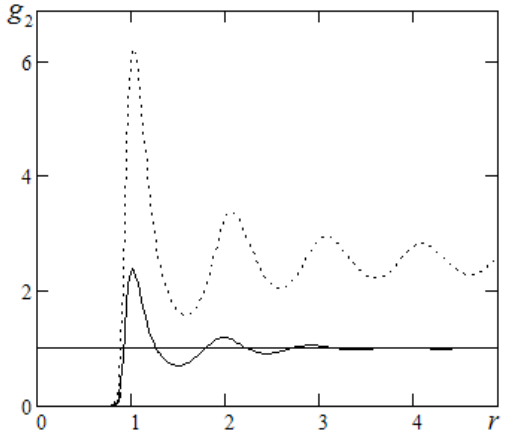

Fig. 2.3. Radial distribution function g_2 in bulk (solid curve) and in a nanochannel at the first density maximum (dashed curve). $h = 6\sigma$, $\varepsilon_V = 0.88$.

Density profiles give local information on the fluid structure. However, an analysis of the Figs. 2.1 and 2.2 shows that the short-range order of the fluid varies in a nanochannel. It should be appreciable at least near the walls. The fluid structure is characterized by the radial distribution function of the molecules. Figure 2.3 shows radial distribution functions in the bulk and at the first density maximum (see Fig. 2.1) in a nanochannel. The distance r is in σ. It is evident that the number and magnitude of the maxima in the channel are significantly larger than those in the open system, indicating an increase in the short-range order in the fluid due to its interaction with the walls. Near the wall, the radial distribution function decays over a distance an order of magnitude larger than in the bulk. In fact, quasi-long-range order is observed near the wall.

3. Diffusion in Nanochannel

As rule, microchannel flows are laminar. Therefore, transfer processes play a special role in such flows. They determine flow mixing, heat exchange with the walls, etc. In this section, we consider the self-diffusion of fluid molecules in plane and rectangular nanochannels. The self-diffusion coefficient was calculated by the Green–Kubo formula

$$D = \frac{1}{3}\int_0^T \chi(t)dt\,, \qquad (3.1)$$

where χ is the velocity autocorrelation function (VACF) of the molecules, which is defined as ($d = x, y, z$)

$$\chi_d(t) = \frac{1}{Nl}\sum_{i=1}^{N}\sum_{j=0}^{l-1}\left[v_{id}(j\Delta t)\cdot v_{id}(j\Delta t + t)\right].$$

T is the time in which the VACF reaches a plateau value (Rudyak et al., 2008). Here N is the number of particles in the cell, l is the number of partitions of the time interval in which the VACF was calculated, and Δt is the integration step.

Simultaneously, the self-diffusion coefficient was determined from Einstein's relation

$$\left\langle R_d^2(t)\right\rangle = \frac{1}{Nl}\sum_{i=1}^{N}\sum_{j=0}^{l-1}\left[r_{id}(j\Delta t) - r_{id}(j\Delta t + t)\right]^2 = 2Dt$$

using calculated values of the mean-square displacement of molecules $< R^2 >$.

To study the self-diffusion of molecules in a nanochannel, we considered HS and LJ fluids and the diffusion of argon molecules in a channel with carbon or silicon walls. It has been found that

- the molecular diffusion in a nanochannel is not isotropic;
- in plane channels, the diffusion coefficients along the x and y axes (along the channel) are identical and equal to $D_b/3$, where D_b is the bulk self-diffusion coefficient;

- in small channels, the diffusion coefficient across the cannel (along the *z* axis) is equal to zero;
- in rectangular channels, the diffusion coefficient practically does not depend on the aspect ratio.

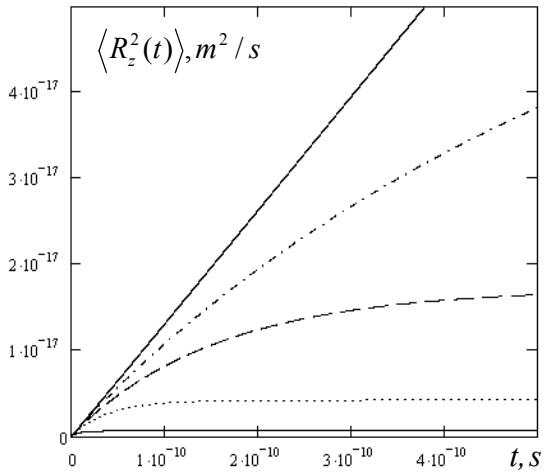

Fig. 3.1. Mean-square displacement of molecules $\langle R_z^2(t)\rangle$ versus the time for various values of *h*. ε_V = 0.257

Physically, these results are quite natural. In a channel of small size, the mean-square displacement is on the order of its height or width, and the diffusion coefficient in this directions tends to zero as $t \to \infty$. Curves of the mean-square displacement of HS molecules along the *z* axis for plane channels are shown in Fig. 3.1. Here the lower curve corresponds to a height *h* = 2 nm, the dotted curve to *h* = 5 nm, the dashed curve to *h* = 10 nm, and the dot-and-dashed curve to *h* = 20 nm. The upper solid straight line is calculated for the bulk. The diffusion coefficient is in the units of $\sigma\bar{v}$, where $\bar{v}$ is the mean thermal velocity of the molecules.

Naturally, the diffusion coefficient decreases as the fluid density increases. The diffusion coefficient is inversely proportional to the fluid density (in the density range studied).

4. Diffusion in Porous Media

The characteristic pore size varies from several tens of nanometers to several tens or even hundreds of micrometers (Nelson, 2009). On these scales, the MD method is, in fact, the only adequate method for simulating transport processes. In the present work, the porous matrix was modeled by cubic packing of spheres of the same radius, and the packing density and the grain size were varied. The calculations were performed in a cell with periodic boundary conditions, i.e., in fact, an infinite porous medium was modeled. The porosity of the matrix $\varphi = V/V_p$, (V_p is the pore volume and V is the total volume of the medium) was varied from 0.5 to 0.9, and the fluid density $n = V_f/V_p$ from 0.07 to 0.565 (V_f is the volume of the fluid molecules). In almost all cases, we studied the self-diffusion of molecules of dense gases or moderately dense gases. At the upper limit, the fluid density is close to the liquid density.

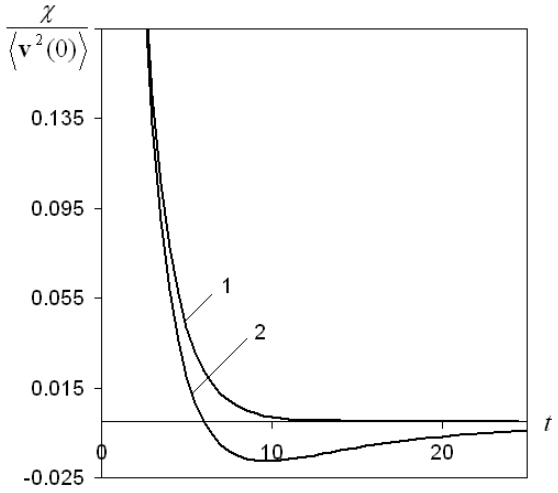

Fig. 4.1. Time dependence of the VACF (in free path times)

The self-diffusion coefficient for the fluid molecules was obtained using the Green–Kubo formula (3.1). Figure 4.1 shows a typical VACF normalized to the mean value of the squared velocity for a fluid of density $n = 0.0707$. Here curve 1 corresponds to the fluid VACF in the bulk and curve 2 in the porous medium. In all the calculations performed, the VACF has a negative well (see Fig. 4.1), whose depth and position depend on the porosity, fluid density, and the size ratio of the fluid molecules to the particles of the porous medium. Unlike in self-diffusion in the bulk, a negative well is also present for rarefied gases. Its occurrence is due to the

interaction of molecules with the solid matrix, whereas in the bulk, this behavior is typical only of liquids and is related to the occurrence of short-range order in the system. A significant change in the VACF of fluid molecules in a porous medium leads to a decrease in the diffusion coefficient compared to its value in the bulk. This is quite natural from a physical point of view; however, it is important to understand what these changes are and how they depend on the parameters of the porous medium and fluid.

One of the most important parameters that determine diffusion in a porous medium is the ratio of the molecular radius of the transported substance r to the particle size of the porous matrix R. The dependence of the self-diffusion coefficient on $\lambda = R/r$ was simulated for various densities, porosities, etc. In all cases, this dependence is well described by the logarithmic law

$$D/D_0 = \alpha \ln \lambda + \beta , \qquad (4.1)$$

where the coefficients α and β depend on the parameters of the system. Hereinafter, the diffusion coefficient is normalized to its value in the bulk D_0. Figure 4.2 shows a typical dependence of the diffusion coefficient on the ratio λ obtained by MD simulation for a HS fluid of density $n = 0.0707$. Here the points are the MD data. These data are well approximated (solid curve) by the relation $D/D_0 = 0.22 \ln \lambda - 0.4$ (see Eq. (4.1)).

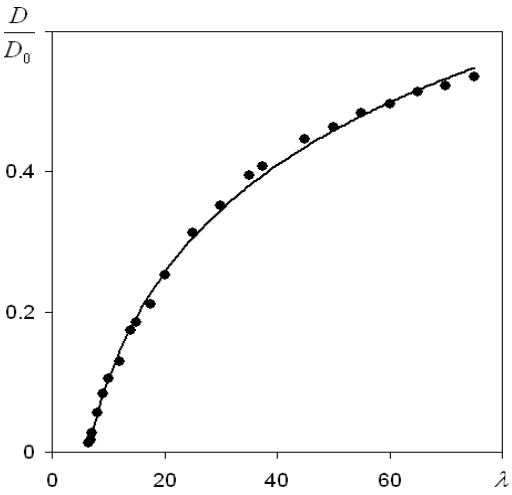

Fig. 4.2. Normalized self-diffusion coefficient versus λ

Previously, dependences of this kind have also been obtained experimentally. A similar dependence was derived in Kim, 2008, where the self-diffusion coefficient of water molecules in a packing of glass spheres was measured using nuclear magnetic resonance (NMR). The size of the spheres was varied from 10 to 600 μm. Immediate comparison of our data with experimental results Kim, 2008 is impossible because in our calculations, self-diffusion was simulated in pores with characteristic sizes of a few to several tens of nanometers, i.e., several orders of magnitude smaller. Nevertheless, the dependences for the self-diffusion coefficient obtained in Kim, 2008 agree qualitatively with Eq. 4.1.

Another important characteristic of the system is its porosity. The porosity formed by packing of hard spheres is naturally related to the grain (sphere) radius of the packing. It is easy to see that $\varphi = 1 - 4\pi n_p R^3/3$, where n_p is the grain density in the skeleton (number of grains in unit volume). Since the dependence of the diffusion coefficient on the grain radius is given by Eq. 4.1, it is obvious that its dependence on the porosity will also be determined by a logarithmic function. This is indeed so; the dependence of the diffusion coefficient on the porosity of the skeleton is given by the relation $D/D_0 = \gamma \ln \varphi + 1$, where γ is a coefficient that depends on the parameters of the system considered. In particular, for a fluid with $n = 0.0707$ and $\lambda = 25$, this dependence has the form

$$D/D_0 = 0.984 \ln \varphi + 1 . \qquad (4.2)$$

As in the bulk, the self-diffusion coefficient of the fluid depends significantly on its density. The dependence of the self-diffusion coefficient on the Knudsen number *Kn* is linear for various ratios of the radii and porosities ($Kn = l/R$, where l is the mean free path length of the molecules). This behavior of the self-diffusion coefficient is typical of ideal gases; in this case, the linear dependence of D on *Kn* should correspond to an inversely proportional dependence of the self-diffusion coefficient on fluid density. Indeed, the simulation results show that

$$D/D_0 = \alpha / n , \qquad (4.3)$$

where α is a coefficient that depends on the parameters of the system. Figure 4.3 shows the

dependence of the self-diffusion coefficient on the fluid density for $\lambda = 25$ and $\varphi = 0.5$. Here the points are MD simulation data, and the solid curve corresponds to Eq. 4.3. For the specified values of the matrix parameters, $\alpha = 2.66$.

It should be noted that the difference between the self-diffusion coefficient in a porous medium and the corresponding bulk value is significantly larger for less dense fluids than for dense fluids. This is due to an increase in the contributions of interactions of fluid molecules with the porous medium to the total number of interactions.

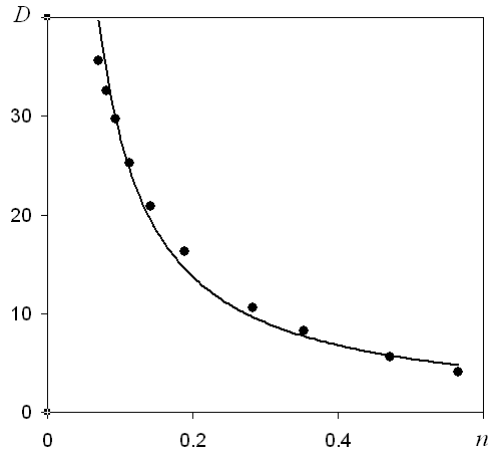

Fig. 4.3. Normalized self-diffusion coefficient versus fluid density

In accordance with Eq. 3.1, the self-diffusion coefficient depends on time. A comparison of a typical time dependence of the self-diffusion coefficient $D(t)$ for porous media with $D_0(t)$ is presented in Fig. 4.4. The diffusion coefficient in the bulk increases steadily and reaches a plateau value which is the actual value of the diffusion coefficient in the bulk. In porous media, the function $D(t)$ is not monotonic. This function first increases to reach a maximum and then decreases. In porous media, a plateau value is also reached, but it is determined by the porosity of the medium and is lower than the corresponding value in the bulk (cf. the two curves in Fig. 4.4). As a rule, the time dependence of the self-diffusion coefficient at short times is studied using NMR measurements. At such times, the molecule displacement is smaller then the pore size. However, on these scales, the behavior of the function $D(t)$ changes sharply (as can be seen in Fig. 4.4.) i.e., the mean-square displacement of a molecule is not described by the well-known Einstein–Langevin formula ($< R^2 > \sim t$). Thus, one must be careful in interpreting NMR data.

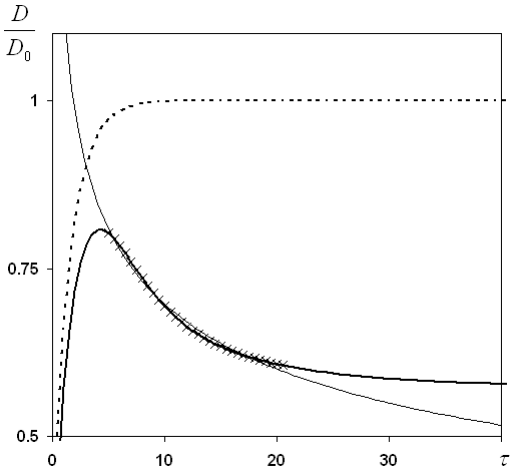

Fig. 4.4. Normalized self-diffusion coefficient versus time (in free path times). The solid curve corresponds to a porous medium ($\varphi = 0.5$, $\lambda = 25$, $n = 0.0707$) and the dotted curve to the bulk

The short-time branch of the diffusion coefficient curve, marked by crosses in Fig. 4.5, is described by the formula $D/D_0 \sim t^{-0.22}$. In this case the mean-square displacement of molecules is determined by the relation: $\langle R^2 \rangle \sim t^{0.78}$. Thus, short-time diffusion which is generally measured by NMR is not classical. This is so-called sub-diffusion $\langle R^2 \rangle \sim t^{\alpha}$, where the parameter $\alpha < 1$ and depends on the fluid density and porosity.

5. Fluid Viscosity in Nanochannels

Change in the fluid structure in nanochannels should have a significant effect on transfer processes in them. The change in the structure leads to several consequences that should be taken into account in studying and modeling the transport processes. First, the change in the fluid structure should change the equation of state of the fluid. Therefore, the

equality of the pressures and temperatures of fluids in a channel and the bulk does not imply that their densities are equal. Second, the determination of fluid density in nanochannels requires great care. This is due to the fact that near the walls there are screening zones. Therefore, if the physical volume of a nanochannel is equal to V, the volume available for HS fluid molecules $\widetilde{V} < V$. On the other hand, for LJ molecules there is the opposite (though insignificant) effect, where fluid molecules are introduced into the molecular lattice of the channel walls. As a result, at a given pressure and temperature, the fluid densities in the bulk and in nanochannels are different. In practice, the quantities measured in microchannels and nanochannels are usually pressure and temperature. Therefore, in the present work, fluid viscosities in the bulk and in nanochannels were compared at given pressure and temperature.

Finally, it should be noted that fluid structuring in nanochannels disturbs its homogeneity (see Fig. 2.2), and the transport processes are no longer isotropic. The viscosity coefficient is given by the relation

$$\eta = (\eta_{xy} + \eta_{xz} + \eta_{yz})/3, \qquad (5.1)$$

where the contributions are calculated by Green–Kubo type formulas

$$\eta_{\alpha\beta} = \frac{1}{5}\int_0^T \chi_{\alpha\beta}(t)dt, \quad \alpha,\beta = x,y,z, \quad \alpha \neq \beta,$$

and $\chi_{\alpha\beta}$ are the corresponding correlation functions.

For definiteness, let the z axis is directed across the channel and let periodic boundary conditions be imposed along the x and y axes. Then the coefficients η_{xz} and η_{yz} are equal to each other, and the coefficient η_{xy} is close to the value observed in the bulk.

This paper gives data of a systematic MD simulation of the shear viscosity of a LJ fluid (argon) in a plane channel with carbon (σ = 3.4 Å, ε/k_B = 28 K) or silicon (σ = 3.826 Å, ε/k_B = 202.45K) walls. The viscosity coefficient of the fluid η in the channel was compared with its value η_0 in the bulk. The bulk fluid density was $\varepsilon_V = 0.9$. The fluid density in the channel was determined from the condition of equal pressures of the fluid in the channel and in the bulk. In the channel with the carbon walls, $\varepsilon_V = 0.9$, and in the channel with silicon walls, ε_V = 0.912 for a channel height $h = 18\sigma$ and ε_V = 0.936 for $h = 6\sigma$.

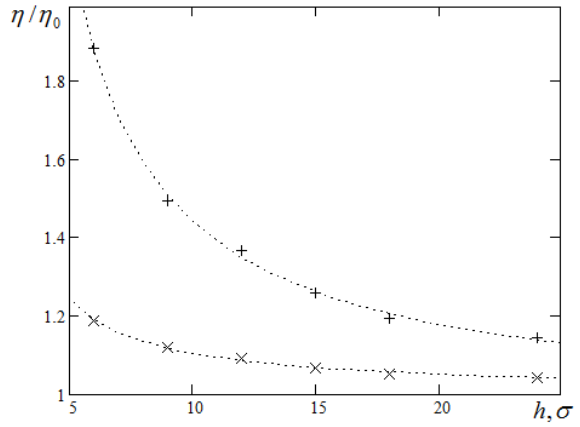

Fig. 5.1. Viscosity coefficient of argon versus distance between the walls of carbon molecules (×) and silicon molecules (+) at T = 200 K

The dependence of the viscosity coefficient (5.1) on the height of the channel is shown in Fig. 5.1. As expected, the viscosity coefficient increases with decreasing channel height. However, this increase depends greatly on the material of the walls. In the channel with silicon walls, the viscosity increases more significantly.

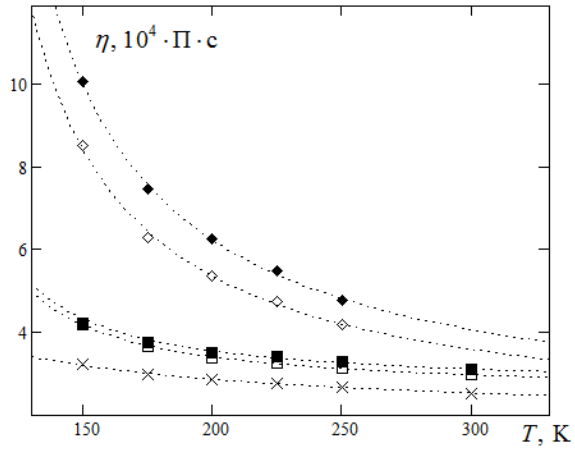

Fig. 5.2. Argon viscosity versus temperature in the bulk (×), in the channel with carbon walls (□), and with silicon walls (◊)

The temperature dependence of viscosity is shown in Fig. 5.2. Here open symbols correspond to the total value of the viscosity coefficient, and filled symbols to the viscosity in the plane perpendicular to the channel walls. Increasing the temperature leads to a decrease in the viscosity in both the open system and in the channel. However, in the channel, the rate of this decrease is higher, and the effects of the channel walls on viscosity will therefore be more pronounced at low temperatures.

Conclusions

Current studies of transport processes in microchannels and nanochannels are the first steps toward an understating of these phenomena. MD simulation data on the viscosity and self-diffusion coefficients in nanochannels and in a porous medium show that the most important factor in these processes is the interaction between fluid molecules and the channel walls (porous medium) and the change in the fluid structure. In a microchannel, the fluid short-range order, (which largely determines, e.g., the fluid viscosity) changes at the channel wall.

In nanochannels, fluid structuring is of fundamental importance. However, the interaction with the boundary leads to a pressure drop along the channel. Accordingly, the fluid structure will vary along the channel. If the channel fluid temperature does not change, the pressure drop along the channel implies a decrease in the fluid density. Fluids in nanochannels are always compressible. Therefore, generally speaking, the transfer coefficients vary along the channel and one can introduce only some averaged transfer coefficients.

Finally it should be noted that in determining the fluid density in nanochannels, one should take into account the presence of screening zones near the channel walls. This effect becomes negligible in channels where $h \geq 100\sigma$.

Acknowledgments

This work was supported in part by the Russian Foundation for Basic Research (Grant No. 10-01-00074) and the Federal Special Program “Scientific and scientific-pedagogical personnel of innovative Russia in 2009-2013” (projects No. P230 and No. 14.740.11.0579, No. 14.740.11.0103).

References

Kang, Y.J., Yoon, S.Y., Yang, S., 2010. Viscosity measurement using hydrodynamic divergencing chamber and digital counting in microfluidic channels. In: Proceedings of the IEEE Int. Conf. on MEMS, Hong Kong, Paper no. 5442562, 71–74.

Kärger, J., Ruthven, D.M., 1992. Diffusion in zeolites and over microporous solids. John Wiley & Sons, New York.

Kim, K.H., 1998. Experimental Measurement of Restricted Diffusion. Chemical Industry and Technology 16 (6), 562–567.

Latour, L.L., Mitra, P.P., Kleinberg, R.L., Sotak, C.H., 1993. Time-dependent diffusion coefficient of fluids in porous media as a probe of surface-to-volume ratio. J. Magn. Reson. Series A101, 342–346.

Nelson, P.H., 2009. Pore-throat sizes in sandstones, tight sandstones, and shales. AAPG Bulletin 93 (3), 329–340.

Rudyak, V.Ya., Belkin, A.A., Ivanov, D.A., Egorov, V.V., 2008. Molecular dynamics simulation of transport processes: The self-diffusion coefficient. High Temperature 46 (1), 30–39.

Song, Y.Q., Ryu, S., Sen, P.N., 2000. Determining multiple length scales in rock. Nature 406, 178–181.